

Computationally Efficient Robust Beamforming for SINR Balancing in Multicell Downlink

Muhammad Fainan Hanif, Le-Nam Tran, *Member, IEEE*, Antti
Tölli, *Member, IEEE*, and Markku Juntti, *Senior Member, IEEE*

Abstract

We address the problem of downlink beamformer design for signal-to-interference-plus-noise ratio (SINR) balancing in a multiuser multicell environment with imperfectly estimated channels at base stations (BSs). We first present a semidefinite program (SDP) based approximate solution to the problem. Then, as our main contribution, by exploiting some properties of the robust counterpart of the optimization problem, we arrive at a second-order cone program (SOCP) based approximation of the balancing problem. The advantages of the proposed SOCP-based design are twofold. First, it greatly reduces the computational complexity compared to the SDP-based method. Second, it applies to a wide range of uncertainty models. As a case study, we investigate the performance of proposed formulations when the base station is equipped with a massive antenna array. Numerical experiments are carried out to confirm that the proposed robust designs achieve favorable results in scenarios of practical interest.

Index Terms

SINR balancing, massive MIMO, very large-scale antenna arrays, reduced complexity, interference channel, multicell beamforming.

I. INTRODUCTION

In practical wireless systems, it is virtually impossible to provide an error-free estimate of channel state information (CSI) to the transmitter. Although beamforming is very attractive from implementation and performance perspective, its applicability is reduced due to its sensitivity to channel estimation errors which may arise as a consequence of pilot contamination in multicell systems [1], quantization effects due to digital processing [2] etc. Motivated by this dilemma, various studies have been conducted to design ‘uncertainty immune’ precoders, see e.g., [3]–[6]

The authors are with the Department of Communications Engineering and Centre for Wireless Communications, University of Oulu, Finland. Email: {mhanif, ltran, atolli, markku.juntti}@ee.oulu.fi.

and references therein. The key tool common to all the studies is the application of various important results from the robust optimization theory [7], [8]. For any optimization problem, the design of robust counterpart can potentially suffer from two major difficulties, namely, (i) hurdles in obtaining tractable representation of the robust counterpart of the original program thereby compelling to employ various approximations, and, (ii) once a tractable formulation is obtained an increase in the complexity of the robust counterpart is seen as compared to the original problem. This pattern is common to most robust designs pertaining to signal processing and communication applications in the literature.

The significance of (ii) in designing uncertainty immune precoders is further enhanced when some of the parameters involved in the system setup take very large values. In this context, the recently envisaged large scale massive multiple-input multiple-output (MIMO) systems [9] can be considered. Indeed, such large-scale antenna arrays promise increased link reliability, better spectral efficiency and low power consumption at the cost of manifold increase in the number of transmitter antennas compared with the traditional multiple-antenna systems. For instance, values of the order of hundreds of base station antennas have been proposed in [9]. The sub-optimality of traditional precoding methods like zero-forcing, block-diagonalization is now well understood [10]. Any algorithm that is, for example, based on traditional mathematical programming is likely to outperform the heuristic approaches of zero-forcing etc. It is also pertinent to point out that the mathematical analysis of the present paper can be easily leveraged to the case of maximizing weighted sum rates based on the development presented in [10]. The traditional approaches of introducing robustness in the the precoder design can end up in a semidefinite program (SDP). The complexity of an SDP is highly sensitive to the precoder size (more details on this appear in Sec. III-B), and hence the SDP-based solutions can either incur appreciable computational cost or in certain circumstances the digital resources may not be sufficient to cater for the memory requirements of an SDP-based solution. On the other hand, second-order cone programs (SOCPs) are much more computationally efficient (again the details appear in Sec. III-B), and can certainly provide a viable alternative to designing algorithms for very large-scale antenna arrays. This motivates arriving at robust SOCP formulations for optimizing certain performance metric in modern communication systems.

In this paper, we study the problem of signal-to-interference-plus-noise ratio (SINR) balancing in multicell multiple-input single-output (MISO) downlink or interfering broadcast channel with

a realistic assumption of imperfect CSI. We focus on centralized base station (BS) control. The worst case design philosophy that is commonly employed in the existing literature is considered. We first show that the robust counterpart can be relaxed to an SDP, and, thus, can be (suboptimally) solved in conjunction with a bisection search. It appears that the SDP-based formulations provide a general solution to the robust design in many works, e.g., [4]–[6]. However, the SDP-based methods may rely on a rank relaxation scheme, which is in general a suboptimal technique. Furthermore, the SDP-based approaches generally result in computationally expensive tractable robust counterparts. As our main contribution, we propose a robust design which is merely based on solving SOCPs, i.e., the proposed method does not represent much increase in complexity in comparison to the original version of the SINR balancing problem. This is accomplished by exploiting various properties of the constraints in the robust counterpart of the balancing problem. In particular, we avoid formulating the beamformer design by projecting it to the space of semidefinite matrices which normally results in a rank constrained SDP. More importantly, the proposed SOCP-based design can be used in a wide range of uncertainty models. We notice that the SDP-based design formulations commonly used in literature [4]–[6] are only applicable to the cases where the channel errors lie in an ellipsoid. As mentioned above, we also compare and contrast the SDP and SOCP solutions, particularly from the computational cost perspective, when the number of base station antennas is very large [9]. Finally, through numerical investigations, we show that the proposed SOCP-based solution offers comparable performance to the approach in [6] and the SDP-based method when same uncertainty set (a ball) is used to represent channel perturbations.

The rest of the paper is organized as follows. Section II presents problem formulation, a solution for perfect CSI, and modeling of the balancing problem with imperfect CSI. Section III discusses in detail various solutions with imperfect CSI along with a comparative discussion about their properties. Finally, Sections IV and V describe numerical experiments and conclusions, respectively.¹

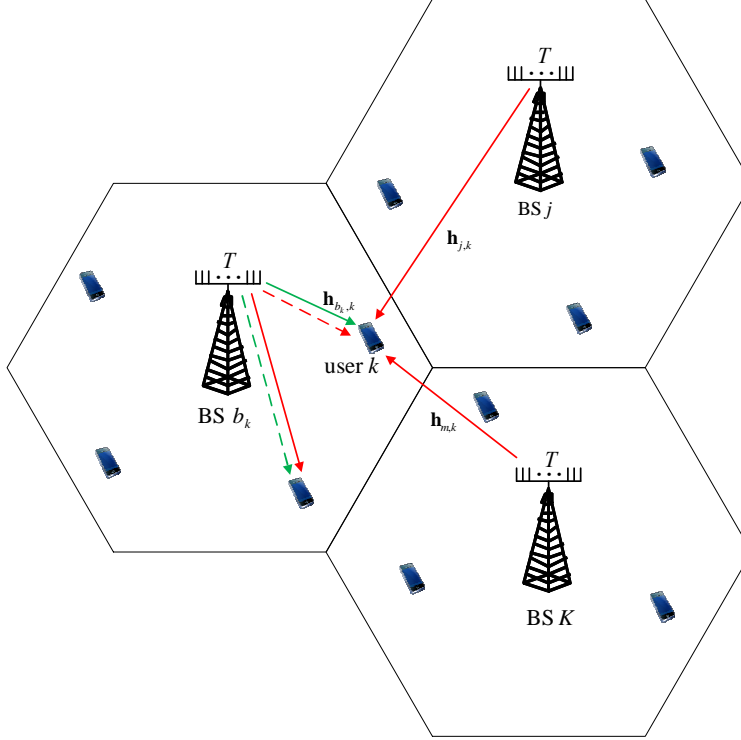


Fig. 1. System model of a multicell MISO downlink channel. Green lines represent desired signals, while red ones denote interference. The serving base station for user k is denoted by b_k .

II. SYSTEM MODEL

Consider a system of B coordinated BSs and K users where each user is served by one BS. Each BS is equipped with T transmit antennas and each user with a single receive antenna. A sketch of the system model is presented in Fig. 1. Interference originating outside the coordinated system is omitted. The serving BS for the k th user is denoted by b_k . The signal received by the k th user is

$$y_k = \mathbf{h}_{b_k,k} \mathbf{x}_k + \sum_{i=1, i \neq k}^K \mathbf{h}_{b_i,k} \mathbf{x}_i + n_k \quad (1)$$

where $\mathbf{h}_{b_k,k} \in \mathbb{C}^{1 \times T}$ is the channel (row) vector from BS b_k to user k , $\mathbf{x}_k \in \mathbb{C}^{T \times 1}$ is the transmitted signal vector from the BS b_k to user k and $n_k \sim \mathcal{CN}(0, \sigma^2)$ represents circularly

¹We use bold lowercase letters to express vectors and bold uppercase letters to represent matrices. $(\cdot)^H$, $(\cdot)^T$ and $\text{Tr}(\cdot)$ represent the Hermitian, transpose and the trace operators, respectively. $\mathbb{C}^{a \times b}$ and $\mathbb{R}^{p \times q}$ represent the space of complex and real matrices (vectors) of dimensions given as superscripts, respectively. $|\mathcal{M}|$ denotes the cardinality of set \mathcal{M} . $[\mathbf{p}]_k$ represents the k th component of vector \mathbf{p} . $|c|$ and $\Re(c)$ represent the absolute value and the real part of a complex number c , respectively. \mathbf{I}_T denotes a $T \times T$ identity matrix. Finally, $\|\cdot\|_2$ represents the l_2 norm.

symmetric zero mean complex Gaussian noise with variance σ^2 . The transmitted signal vector is defined as $\mathbf{x}_k = \mathbf{m}_k d_k$, where $\mathbf{m}_k \in \mathbb{C}^{T \times 1}$ is the unnormalized beamforming vector and d_k is the normalized complex data symbol. The total power transmitted by BS b is $\sum_{k \in \mathcal{U}_b} \text{Tr}(\mathbb{E}[\mathbf{x}_k \mathbf{x}_k^H]) = \sum_{k \in \mathcal{U}_b} \|\mathbf{m}_k\|_2^2$, where the set \mathcal{U}_b with size $K_b = |\mathcal{U}_b|$ includes the indices of all users served by BS b . The SINR at user k 's receiver is

$$\gamma_k = \frac{|\mathbf{h}_{b_k, k} \mathbf{m}_k|^2}{\sigma^2 + \sum_{i \in \mathcal{U}_{b_k} \setminus k} |\mathbf{h}_{b_k, k} \mathbf{m}_i|^2 + \sum_{b=1, b \neq b_k}^B \sum_{i \in \mathcal{U}_b} |\mathbf{h}_{b, k} \mathbf{m}_i|^2} \quad (2)$$

where the interference power in the denominator is divided into intra- and inter-cell interference components.

A. Problem Statement and Solution for Perfect CSI

For the case of perfect CSI, the maximin SINR balancing can be cast as

$$\underset{\mathbf{m}_k: \sum_{k \in \mathcal{U}_b} \|\mathbf{m}_k\|_2^2 \leq P_b, \forall b}{\text{maximize}} \quad \min_k \alpha_k \gamma_k \quad (3)$$

where α_k are positive weighting factors. Using (2), we can equivalently reformulate (3) as

$$\begin{aligned} & \underset{\mathbf{m}_k, t}{\text{maximize}} \quad t \\ & \text{subject to} \quad \|(\mathbf{h}_{1, k} \mathbf{M}_1 \cdots \mathbf{h}_{B, k} \mathbf{M}_B \sigma)^H\|_2 \leq \sqrt{1 + \frac{\alpha_k}{t}} |\mathbf{h}_{b_k, k} \mathbf{m}_k|, \quad \forall k, \\ & \quad \|\text{vec}(\mathbf{M}_b)\|_2 \leq \sqrt{P_b}, \quad \forall b. \end{aligned} \quad (4)$$

where $\mathbf{M}_b = [\mathbf{m}_{\mathcal{U}_b(1)}, \dots, \mathbf{m}_{\mathcal{U}_b(|\mathcal{U}_b|)}]$ includes the precoders of all users being served in the b th cell and the operation $\text{vec}(\cdot)$ vectorizes the argument matrix by stacking columns. Furthermore, we can still find an optimal solution of (4) even if $\mathbf{h}_{b_k, k} \mathbf{m}_k$, for all k , is forced to be real [3], [11], [12]. In this way, the constraints in (4) represent second order cone (SOC) constraints for fixed t . Therefore, the original problem can be solved as a series of SOCP feasibility problems using bisection search [11], [13].

B. Modeling of Imperfect CSI

In real systems it is impossible to achieve perfect transmitter CSI due to several reasons mentioned in, e.g., [5], [6]. Hence, robust designs dealing with channel errors are of practical importance. We consider the channel uncertainty model in which the true channel vectors are

of the form

$$\mathbf{h}_{b,k} = \hat{\mathbf{h}}_{b,k} + \sum_{i=1}^{l_{b,k}} \delta_{b,k}^i [\mathbf{v}_{b,k}]_i = \hat{\mathbf{h}}_{b,k} + \mathbf{v}_{b,k} \mathbf{A}_{b,k}, \quad \forall b, k \quad (5)$$

where $\hat{\mathbf{h}}_{b,k}$ represents the nominal (known) value of the channels, $l_{b,k} \in \{1, 2, \dots, T\}$, the vectors $\delta_{b,k}^i$ (channel perturbation directions) form the rows of $\mathbf{A}_{b,k} \in \mathbb{C}^{l_{b,k} \times T}$ and $\mathbf{v}_{b,k} \mathbf{A}_{b,k}$ gives the error vector in the downlink channel from BS b to user k [7], [14]. We denote by \mathcal{S} the uncertainty set that includes all channel error row vectors $\mathbf{v}_{b,k}$. As seen in (5) the above model assumes that the uncertainty vector affects the data in an affine manner. This philosophy has been widely used, e.g., in [5], [6] etc. In addition to affecting the true channels in an affine manner, the error vectors are also constrained to lie in an uncertainty set $\mathcal{S}_{b,k}$ as

$$\mathcal{S}_{b,k} = \{\mathbf{v}_{b,k} : \|\mathbf{v}_{b,k}\| \leq \rho_{b,k}, \forall b, k\} \quad (6)$$

where $\|\cdot\|$ is an appropriate norm specified by the parameter $\rho_{b,k}$, and is chosen based on how one wishes to model channel uncertainties. Normally, modeling channel errors by exploiting their statistical nature is prone to numerous difficulties. To name a few, it requires information about the statistics of the error vectors which is mostly not available on account of myriad of phenomenon involved in the channel estimation process. Then even if some information about the statistics of the error vectors is exploitable, a part from simple linear constraints contaminated with Gaussian errors, it is virtually impossible to arrive at exact tractable versions of *stochastic constraints*. Motivated by the dilemma, the uncertainty in channels is modeled by norm-bounded sets (6). With such modeling, it does not remain necessary to know information about the, say, probability law that the uncertainty vectors follow. Further to this, as we will see in the discussion to follow, norm-bounded uncertainty sets model various real world scenarios very well. One more advantage of such modeling is that in several cases of interest, the norm-bounded uncertainty models permit either exact tractable formulations or good approximations [14], [15].

C. Worst Case Design Formulation

We will concentrate on the worst case robust optimization approach of [8], [14] that has been traditionally used in the existing literature for different problems [4]–[6]. The worst case approach amounts to satisfying the constraints for all possible channel vectors. Hence, the robust

counterpart of (3) is written as

$$\begin{aligned}
& \max_{\mathbf{m}_k, t} t \\
& \text{s. t.} \quad \frac{\alpha_k}{t} |\mathbf{h}_{b_k, k} \mathbf{m}_k|^2 \geq \sum_{i \in \mathcal{U}_{b_k} \setminus k} |\mathbf{h}_{b_k, k} \mathbf{m}_i|^2 + \sum_{b=1, b \neq b_k}^B \sum_{i \in \mathcal{U}_b} |\mathbf{h}_{b, k} \mathbf{m}_i|^2 + \sigma^2, \forall k, \forall \{\mathbf{v}_{b, k} \mathbf{A}_{b, k} : \mathbf{v}_{b, k} \in \mathcal{S}_{b, k}\} \\
& \quad \sum_{k \in \mathcal{U}_b} \|\mathbf{m}_k\|_2^2 \leq P_b, \forall b.
\end{aligned} \tag{7}$$

We note that the formulation in (7) is intrinsically intractable owing to its semi-infinite nature i.e., finite optimization variables and infinite constraints.

Remark 1: It is worth mentioning here that for the case of receivers equipped with multiple antennas (and hence the possibility of transmitting multiple data streams), an option could be to employ receiver combining matrix and study the balancing problem on per stream basis. The problem is then exactly similar to our case for a given receiver processing matrix per user. Here we stress that even in the presence of perfect CSI, joint transmitter-receiver processing matrix design is a difficult nonconvex problem.

III. ROBUST BEAMFORMER DESIGNS FOR IMPERFECT CSI

A. SDP-Based Robust Design

The solution to problem (7) significantly depends on the type of the uncertainty set. In the context of SDP design, the most commonly considered uncertainty model is the one where error vectors $\mathbf{v}_{b, k}$ are bounded in a ball of radius $\rho_{b, k}$, i.e., $\mathcal{S}_{b, k}$ is expressed as

$$\mathcal{S}_{b, k} = \{\mathbf{v}_{b, k} : \|\mathbf{v}_{b, k}\|_2 \leq \rho_{b, k}, \forall b, k\}. \tag{8}$$

It is clear from (5) and (8) that $\mathbf{h}_{b, k}$ is assumed to lie in an ellipsoid centered at $\hat{\mathbf{h}}_{b, k}$, which is characterized by $\rho_{b, k}$ and $\mathbf{A}_{b, k}$. This type of channel error model is commonly known as ellipsoidal uncertainty model in the related literature. For practical channel estimation schemes it is known that the channel estimation error follows Gaussian distribution [16]. Most of the probability content of multi-dimensional Gaussian density is localized in its certain region. This clearly motivates modeling the error using an ellipsoid. Further, when vector quantization is used at the receiver, quantization errors can also be approximated by ellipsoids [17]. For this specific uncertainty set, we will show that the robust counterpart in (7) can be solved using SDP approximations. We note that in (7) the uncertain part of $\mathbf{h}_{b_k, k}$ varies in the same set on both

sides of the inequality. It is well known that this renders the problem intractable [4], [8], [15]. However, we will see that, after a suitable relaxation, this constraint can be written in a tractable form. To this end, we define $\mathbf{P}_k = \mathbf{m}_k \mathbf{m}_k^H$, $\mathbf{Q}_b = \sum_{k \in \mathcal{U}_b} \mathbf{P}_k$ and $\mathbf{W}_k = \frac{\alpha_k}{t} \mathbf{P}_k - \sum_{i \in \mathcal{U}_{b_k} \setminus k} \mathbf{P}_i$. Then by using slack variables we observe that the constraints involving perturbed channels can be cast into tractable linear matrix inequalities (LMIs) using the so called \mathcal{S} -Lemma or \mathcal{S} -Procedure [8], [18]. After some manipulations, (7) can be equivalently rewritten as

$$\begin{aligned} & \underset{\mathbf{P}_k, t_{b,k}, \lambda_{b,k}, \tau_k}{\text{maximize}} && t \\ & \text{subject to} && \begin{pmatrix} \mathbf{A}_{b_k,k} \mathbf{W}_k \mathbf{A}_{b_k,k}^H + \lambda_{b_k,k} \mathbf{I} & \mathbf{A}_{b_k,k} \mathbf{W}_k \hat{\mathbf{h}}_{b_k,k}^H \\ \hat{\mathbf{h}}_{b_k,k} \mathbf{W}_k \mathbf{A}_{b_k,k}^H & \hat{\mathbf{h}}_{b_k,k} \mathbf{W}_k \hat{\mathbf{h}}_{b_k,k}^H - \tau_k - \lambda_{b_k,k} \rho_{b_k,k}^2 \end{pmatrix} \succeq 0, \forall k \end{aligned} \quad (9a)$$

$$\begin{aligned} & \begin{pmatrix} -\mathbf{A}_{b,k} \mathbf{Q}_b \mathbf{A}_{b,k}^H + \lambda_{b,k} \mathbf{I} & -\mathbf{A}_{b,k} \mathbf{Q}_b \hat{\mathbf{h}}_{b,k}^H \\ -\hat{\mathbf{h}}_{b,k} \mathbf{Q}_b \mathbf{A}_{b,k}^H & -\hat{\mathbf{h}}_{b,k} \mathbf{Q}_b \hat{\mathbf{h}}_{b,k}^H + t_{b,k} - \lambda_{b,k} \rho_{b,k}^2 \end{pmatrix} \succeq 0 \forall k, b \neq b_k \end{aligned} \quad (9b)$$

$$\sum_{k \in \mathcal{U}_b} \text{trace}(\mathbf{P}_k) \leq P_b, \forall b, \quad \sum_{b=1, b \neq b_k}^B t_{b,k} + \sigma^2 \leq \tau_k, \tau_k \geq 0 \forall k \quad (9c)$$

$$\lambda_{b,k} \geq 0 \forall b, k, \quad t_{b,k} \geq 0 \forall k, b \neq b_k, \quad \mathbf{P}_k \succeq 0, \text{rank}(\mathbf{P}_k) = 1 \forall k. \quad (9d)$$

Therefore, after ignoring the nonconvex rank constraints, bisection search over t can be used to obtain covariance matrices. However, we cannot guarantee optimality (see [19]) of the proposed solution if we obtain the rank of precoding matrices greater than unity. Similar rank relaxation approach was also adopted in the recent works, e.g., [5]. We may need some randomization procedure [20] to extract the beamformer \mathbf{m}_k if $\text{rank}(\mathbf{P}_k) > 1$. Nonetheless, randomization trick may not always be useful [5].

B. SOCP-Based Robust Scheme

The robust counterpart of any optimization problem can potentially pose two issues, one related to its tractability, and the other related to its complexity. Very often, the worst case principle leads to an intractable problem, since, as noted previously, the robust counterpart is an optimization problem over an infinite set of constraints. Furthermore, commonly employed approximation schemes usually increase the complexity of the original problem by one degree, i.e., a linear program becomes an SOCP and an SOCP transforms to an SDP. In what follows, we propose a robust design which is merely based on iteratively solving SOCPs, i.e., we attempt

to minimize the complexity of the robust version of the balancing problem. Interestingly enough, we note that the SOCP-based scheme can also encompass a wide variety of uncertainty sets. In order to emphasize the capability of the SOCP scheme to handle a variety of uncertainty sets, we will not specify any particular norm to represent the uncertainty set.

We will arrive at a reduced complexity tractable robust scheme by incorporating uncertainty and exploiting the structure of the SOC constraints in (4). To start with, we consider a relaxation of (7), which is written as

maximize t

subject to

$$C_k \Re \left(\left[\hat{\mathbf{h}}_{b_k,k} + \sum_{i=1}^{l_{b_k,k}} \delta_{b_k,k}^i [\mathbf{v}_{b_k,k}]_i \right] \mathbf{m}_k \right) - \|(z_{1,k} \dots z_{B,k} \sigma)^T\|_2 \geq 0, \forall k, \\ \forall \mathbf{v}_{b_k,k} : \|\mathbf{v}_{b_k,k}\| \leq \rho_{b_k,k} \quad (10a)$$

$$z_{b,k} - \left\| \mathbf{M}_b^H \left[\hat{\mathbf{h}}_{b_k,k} + \sum_{i=1}^{l_{b,k}} \delta_{b,k}^i [\mathbf{v}_{b,k}]_i \right]^H \right\|_2 \geq 0, \forall b, k, \\ \forall \mathbf{v}_{b,k} : \|\mathbf{v}_{b,k}\| \leq \rho_{b,k}, \quad (10b)$$

$$z_{b,k} \geq 0, \forall b, k, \quad \|\text{vec}(\mathbf{M}_b)\|_2 \leq \sqrt{P_b}, \quad \forall b, \quad (10c)$$

where $C_k = \sqrt{1 + \frac{\alpha_k}{t}}$, $\mathbf{m}_k \in \mathbb{C}^{T \times 1}$, $z_{b,k} \in \mathbb{R}$, $\mathbf{M}_b = [\mathbf{m}_{\mathcal{U}_b(1)}, \dots, \mathbf{m}_{\mathcal{U}_b(|\mathcal{U}_b|)}]$ are optimization variables and we have removed the absolute value, and only consider the real part of the left side of the constraints in (10a). Unlike the non-robust version of the problem (4), we cannot force the imaginary part of $[\hat{\mathbf{h}}_{b_k,k} + \sum_{i=1}^{l_{b_k,k}} \delta_{b_k,k}^i [\mathbf{v}_{b_k,k}]_i] \mathbf{m}_k$ to zero for all channel error realizations. Since for a complex number x , $|x| \geq \Re(x)$, a feasible point for (10a) is also feasible for the exact robust counterpart given in (7). That is to say, to arrive at a reduced complexity approach, we consider a conservative approximation of the exact robust counterpart of the problem. For notational simplicity, when clear from context, we avoid mentioning the real operator $\Re(\cdot)$ explicitly from this point onwards.

Now we make a key manipulation by substituting $\mathbf{v}_{b,k} = \boldsymbol{\theta}_{b,k} - \boldsymbol{\phi}_{b,k}$ for all b, k , in (10b) and $\Re(\mathbf{v}_{b_k,k}) = \Re(\boldsymbol{\theta}_{b_k,k}) - \Re(\boldsymbol{\phi}_{b_k,k})$ such that $\Re(\boldsymbol{\theta}_{b_k,k}) \geq 0$ and $\Re(\boldsymbol{\phi}_{b_k,k}) \geq 0$ in (10a). After this

we obtain a relaxation of (10)

maximize t

subject to

$$C_k \left(\Re(\hat{\mathbf{h}}_{b_k,k} \mathbf{m}_k) + \sum_{i=1}^{l_{b_k,k}} \Re(\delta_{b_k,k}^i \mathbf{m}_k) \left(\Re([\boldsymbol{\theta}_{b_k,k}]_i) - \Re([\boldsymbol{\Phi}_{b_k,k}]_i) \right) \right) - \|(z_{1,k} \dots z_{B,k} \sigma)^T\|_2 \geq 0, \forall k,$$

$$\forall \boldsymbol{\theta}_{b_k,k}, \boldsymbol{\Phi}_{b_k,k} : \|\Re(\boldsymbol{\theta}_{b_k,k}) + \Re(\boldsymbol{\Phi}_{b_k,k})\| \leq \rho'_{b_k,k} \quad (11a)$$

$$z_{b,k} - \left\| \mathbf{M}_b^H \left[\hat{\mathbf{h}}_{b,k} + \sum_{i=1}^{l_{b,k}} \delta_{b,k}^i ([\boldsymbol{\theta}_{b,k}]_i - [\boldsymbol{\Phi}_{b,k}]_i) \right] \right\|_2 \geq 0, \forall b, k,$$

$$\forall \boldsymbol{\theta}_{b,k}, \boldsymbol{\Phi}_{b,k} : \|\boldsymbol{\theta}_{b,k}\| + \|\boldsymbol{\Phi}_{b,k}\| \leq \rho'_{b,k}, \quad (11b)$$

$$z_{b,k} \geq 0, \forall b, k, \quad \|\text{vec}(\mathbf{M}_b)\|_2 \leq \sqrt{P_b}, \quad \forall b, \quad (11c)$$

where $[\boldsymbol{\theta}_{b_k,k}]_i, [\boldsymbol{\Phi}_{b_k,k}]_i$ denote the i th components of $\boldsymbol{\theta}_{b_k,k}, \boldsymbol{\Phi}_{b_k,k}$ for all b, k , respectively, and for a vector \mathbf{y} the symbol $|\mathbf{y}|$ represents that $[|\mathbf{y}|]_i = |[y]_i|$ for all i . Another change introduced in (11) is that for all b, k we have replaced $\rho_{b_k,k}$ with $\rho'_{b_k,k}$. The motivation for this variation of the uncertainty set parameter $\rho_{b_k,k}$ becomes clear as we outline the fact that splitting the uncertainty vector $\mathbf{v}_{b_k,k}$ into a difference of two vectors and manipulating the left side of uncertainty sets as done in (11) transforms the problem into *nearly a safe approximation* of its original version while also rendering it *tractability*.

Remark 2: As noted earlier, it appears difficult, if not impossible, to cast the worst case robust counterpart (7) into its exact equivalent tractable formulation. For example, in the first approach based on SDP formulation, we had to drop the unit rank constraints to arrive at a tractable representation. Naturally, to arrive at an SOCP representation of the problem, we have to resort to an approximation of the original feasible set i.e.,

$$\mathcal{O}_{orig} = \{\text{Optimization variables in (7) such that all constraints in (7) are satisfied}\} \quad (12)$$

with its *tractable subset* that may also include some additional analysis variables.

In our case, it should be a feasible set for an SOC problem. By doing so we can ensure that a solution for the approximation is definitely feasible for the original optimization program, and thus promises *safety* in a sense that we do not violate the original constraints. By just considering the real part of the left side of constraints in (10a), we follow this strategy. It is

worthwhile to note that the approximation used in (11a) may compromise safety. However, our numerical investigations in Sec. IV reveal that the safety of the proposed SOCP procedure is almost guaranteed. It is evident that by deriving a subset of the original feasible set, we may have an overly conservative approximation. Hence, manipulating the parameter $\rho_{b,k}$ as $\rho'_{b,k}$ may provide some flexibility to overcome the conservativeness of the proposed approximation [21].

Next, let us first focus on the set of constraints in (11b) and rewrite it in a form similar to the one presented in (10b)

$$z_{b,k} - \left\| \mathbf{M}_b^H \left[\hat{\mathbf{h}}_{b,k} + \sum_{i=1}^{l_{b,k}} \delta_{b,k}^i [\mathbf{v}_{b,k}]_i \right] \right\|_2 \geq 0, \forall b, k, \forall \mathbf{v}_{b,k} : \|\mathbf{v}_{b,k}\| \leq \rho'_{b,k}. \quad (13)$$

It is worthy making an important observation now. A set of optimization variables satisfies the constraints in (11b) if and only if it satisfies the set of constraints in (13). For a given b, k , let us assume that $z_{b,k}$ and \mathbf{M}_b are infeasible in (11b), i.e., there exist $\boldsymbol{\theta}_{b,k}$, $\boldsymbol{\phi}_{b,k}$ and $\| |\boldsymbol{\theta}_{b,k}| + |\boldsymbol{\phi}_{b,k}| \| \leq \rho'_{b,k}$ such that

$$z_{b,k} - \left\| \mathbf{M}_b^H \left[\hat{\mathbf{h}}_{b,k} + \sum_{i=1}^{l_{b,k}} \delta_{b,k}^i ([\boldsymbol{\theta}_{b,k}]_i - [\boldsymbol{\phi}_{b,k}]_i) \right] \right\|_2 < 0. \quad (14)$$

Let $[\mathbf{v}_{b,k}]_i = [\boldsymbol{\theta}_{b,k}]_i - [\boldsymbol{\phi}_{b,k}]_i$ for all i . Thus it is easy to see that $|[\mathbf{v}_{b,k}]_i| \leq |[\boldsymbol{\theta}_{b,k}]_i| + |[\boldsymbol{\phi}_{b,k}]_i|$. Therefore, we obtain $\|\mathbf{v}_{b,k}\| \leq \| |\boldsymbol{\theta}_{b,k}| + |\boldsymbol{\phi}_{b,k}| \| \leq \rho'_{b,k}$, and hence (13) is also infeasible. Next, we assume conversely that for a given b, k , $z_{b,k}$ and \mathbf{M}_b are infeasible in (13), i.e.,

$$z_{b,k} - \left\| \mathbf{M}_b^H \left[\hat{\mathbf{h}}_{b,k} + \sum_{i=1}^{l_{b,k}} \delta_{b,k}^i [\mathbf{v}_{b,k}]_i \right] \right\|_2 < 0 \quad (15)$$

for certain $\mathbf{v}_{b,k}$ such that $\|\mathbf{v}_{b,k}\| \leq \rho'_{b,k}$. Let $[\boldsymbol{\theta}_{b,k}]_i = (1 - \vartheta_{b,k})[\mathbf{v}_{b,k}]_i$ and $[\boldsymbol{\phi}_{b,k}]_i = -\vartheta_{b,k}[\mathbf{v}_{b,k}]_i$, where $\vartheta_{b,k} \in [0, 1]$. With this substitution, it is seen that $[\mathbf{v}_{b,k}]_i = [\boldsymbol{\theta}_{b,k}]_i - [\boldsymbol{\phi}_{b,k}]_i$. Similarly, these substitutions imply $|[\boldsymbol{\theta}_{b,k}]_i| + |[\boldsymbol{\phi}_{b,k}]_i| = |(1 - \vartheta_{b,k})| |[\mathbf{v}_{b,k}]_i| + |-\vartheta_{b,k}| |[\mathbf{v}_{b,k}]_i| = |[\mathbf{v}_{b,k}]_i|$, and, thus, $\| |\boldsymbol{\theta}_{b,k}| + |\boldsymbol{\phi}_{b,k}| \| = \|\mathbf{v}_{b,k}\| \leq \rho'_{b,k}$. Therefore, the variables $z_{b,k}$ and \mathbf{M}_b are infeasible in (11b) as well. Hence, we conclude that the feasibility of the constraints in (11b) implies the feasibility of (13), and vice versa.

The main goal of the development so far is to approximate (11a) and (11b) by SOC constraints so that the resulting robust counterparts in (11a)-(11c) can be cast as an SOCP for fixed t . Since (11a) and (11b) have the same form, it is sufficient to concentrate on tackling the more difficult set of constraints in (11b). We use the concavity of the negative norm to bound (11b) from

below as

$$z_{b,k} - \|\mathbf{M}_b^H \hat{\mathbf{h}}_{b,k}^H\|_2 - \left\| \mathbf{M}_b^H \left[\sum_{i=1}^{l_{b,k}} \delta_{b,k}^i ([\boldsymbol{\theta}_{b,k}]_i - [\boldsymbol{\Phi}_{b,k}]_i) \right]^H \right\|_2 \geq 0, \\ \forall b, k, \forall \boldsymbol{\theta}_{b,k}, \boldsymbol{\Phi}_{b,k} : \|\boldsymbol{\theta}_{b,k}\| + \|\boldsymbol{\Phi}_{b,k}\| \leq \rho'_{b,k}. \quad (16)$$

Again using the concavity argument, the left side of constraints in (16) can be further lower bounded as

$$z_{b,k} - \|\mathbf{M}_b^H \hat{\mathbf{h}}_{b,k}^H\|_2 + \sum_{i=1}^{l_{b,k}} \left[-\|\{\delta_{b,k}^i \mathbf{M}_b\}^H [\boldsymbol{\theta}_{b,k}]_i\|_2 - \|\{\delta_{b,k}^i \mathbf{M}_b\}^H (-[\boldsymbol{\Phi}_{b,k}]_i)\|_2 \right] \geq 0, \forall b, k \\ \forall \boldsymbol{\theta}_{b,k}, \boldsymbol{\Phi}_{b,k} : \|\boldsymbol{\theta}_{b,k}\| + \|\boldsymbol{\Phi}_{b,k}\| \leq \rho'_{b,k}. \quad (17)$$

Reading the inequalities from (17) backwards, and recalling the equivalence of (11b) and (13), we observe that a solution of (17) is also feasible for (13) or (10b).

Remark 3: Before presenting a tractable formulation of the constraints in (17), we again note that the optimal solution of the proposed SOCP relaxation ideally should also be feasible for the original worst case robust counterpart in (7). Therefore, if \mathcal{O}_{socp} represents the feasible set for the SOCP relaxation, then $\mathcal{O}_{socp} \subseteq \mathcal{O}_{orig}$ should hold. This will imply both safety and tractability for the proposed SOCP approximation. Although the transformations that will lead to an SOCP formulation for (17) ensure both these factors, the same cannot be observed for the constraint in (11a). Nevertheless, as also noted above, we will see in Sec. IV that the relation $\mathcal{O}_{socp} \subseteq \mathcal{O}_{orig}$ almost remains valid at least for the cases considered. Being nearly a subset of the original problem, the proposed approximation can be rather conservative, as also noted in [15], [21]. To provide more flexibility in this regard, and as mentioned above, we make $\rho_{b,k}$ a design parameter and replace it by $\rho'_{b,k}$ in (11). With the introduction of this maneuver, we may be able to improve the achieved objective, albeit this may come at the cost of degradation in achieving it for given realizations of channel errors as we probe in the results section.

Let us define

$$f_1(\mathbf{M}_b, z_{b,k}, \hat{\mathbf{h}}_{b,k}) \triangleq z_{b,k} - \|\mathbf{M}_b^H \hat{\mathbf{h}}_{b,k}^H\|_2, \quad f_2(\mathbf{M}_b, \boldsymbol{\delta}_{b,k}^i) \triangleq -\|\{\boldsymbol{\delta}_{b,k}^i \mathbf{M}_b\}^H\|_2. \quad (18)$$

We note that $f_2(\mathbf{M}_b, \boldsymbol{\delta}_{b,k}^i) = f_2(\mathbf{M}_b, -\boldsymbol{\delta}_{b,k}^i)$. With the above definitions and using the fact that

$\|k\mathbf{m}\|_2 = |k|\|\mathbf{m}\|_2$, the constraints in (17) can be equivalently written as

$$f_1(\mathbf{M}_b, z_{b,k}, \hat{\mathbf{h}}_{b,k}) + \min_{\|\boldsymbol{\theta}_{b,k}\| + \|\boldsymbol{\Phi}_{b,k}\| \leq \rho'_{b,k}} \sum_{i=1}^{l_{b,k}} \left\{ f_2(\mathbf{M}_b, \boldsymbol{\delta}_{b,k}^i) |[\boldsymbol{\theta}_{b,k}]_i| + f_2(\mathbf{M}_b, -\boldsymbol{\delta}_{b,k}^i) |[\boldsymbol{\Phi}_{b,k}]_i| \right\} \geq 0. \quad (19)$$

The constraint in (19) can be cast into tractable form using [15, Theorem 1], which is stated as:

Theorem 1: Working in the real domain, given a function $f(\mathbf{x}, \mathbf{U})$ that is concave in data \mathbf{U} for all given \mathbf{x} and scales linearly with the data, we consider a constraint of the following form

$$\min_{\mathbf{u}_1, \mathbf{u}_2 \geq 0: \|\mathbf{u}_1 + \mathbf{u}_2\| \leq \omega} f(\mathbf{x}, \mathbf{U}^n) + \sum_j [f(\mathbf{x}, \boldsymbol{\delta}^j)[\mathbf{u}_1]_j + f(\mathbf{x}, -\boldsymbol{\delta}^j)[\mathbf{u}_2]_j] \geq 0 \quad (20)$$

where \mathbf{U}^n is the nominal part of the data, $\boldsymbol{\delta}^j$ is a vector representing perturbation direction in the j th component of the data and \mathbf{u}_1 and \mathbf{u}_2 are real vectors of appropriate dimensions and the norm in (20) satisfies the property [15, Eq. 6]

$$\|\mathbf{u}\| = \|\|\mathbf{u}\|\| \quad (21)$$

where $\|\mathbf{u}\| = (|u_1|, \dots, |u_d|)$. The constraint (20) admits an equivalent representation of the form $f(\mathbf{x}, \mathbf{U}^n) \geq \omega \|\boldsymbol{\gamma}\|^*$, where $[\boldsymbol{\gamma}]_j = \max\{-f(\mathbf{x}, \boldsymbol{\delta}^j), -f(\mathbf{x}, -\boldsymbol{\delta}^j)\} \geq 0$ and $\|\boldsymbol{\gamma}\|^* \triangleq \max_{\|\mathbf{s}\| \leq 1} \mathbf{s}^T \boldsymbol{\gamma}$ is the dual norm of $\boldsymbol{\gamma}$.

Proof: The proof of the theorem is available in [15, Theorem 1]. However, for the sake of completeness and for demonstrating its applicability on (19) it is relegated to the Appendix. ■

It should be emphasized that the norm in (20) can be arbitrary, as long as it satisfies (21), meaning that the proposed SOCP-based scheme presented next is applicable to a wide variety and combinations of norms and thus uncertainty sets. For the special case of l_2 norm, the norms remain l_2 because of the self dual property of the l_2 norm. Following similar steps used to tackle the constraints in (11b), we can easily see that the uncertain constraints in (11a) can be cast in a form that is amenable to applying Theorem 1. However, some important observations should be re-stressed at this point. Although the constraints in (11a) are linear, the solution of this approximation does not necessarily imply (10a). This differs from the previous scenario where the conversion of the constraints in (10b) to (11b) is safe. Therefore, obtaining a safe, tractable and least possible conservative version of (10a) is left as an open question for future research.

With the aid of Theorem 1, the approximate robust counterpart of the original problem can

be written in the following tractable form

$$\begin{aligned} & \text{maximize} && t \\ & \text{subject to} && C_k \hat{\mathbf{h}}_{b_k,k} \mathbf{m}_k - \left\| \begin{pmatrix} z_{1,k} & \cdots & z_{B,k} & \sigma \end{pmatrix}^T \right\|_2 \geq \rho'_{b_k,k} L_{b_k,k}, \forall k \end{aligned} \quad (22a)$$

$$C_k \boldsymbol{\delta}_{b_k,k}^i \mathbf{m}_k + [\mathbf{q}_{b_k,k}]_q \geq 0, \forall k, q = 1, \dots, l_{b_k,k} \quad (22b)$$

$$- C_k \boldsymbol{\delta}_{b_k,k}^i \mathbf{m}_k + [\mathbf{q}_{b_k,k}]_q \geq 0, \forall k, q = 1, \dots, l_{b_k,k}, \quad \|\mathbf{q}_{b_k,k}\| \leq L_{b_k,k}, \forall k \quad (22c)$$

$$z_{b,k} - \|\mathbf{M}_b^H \hat{\mathbf{h}}_{b,k}\|_2 \geq \rho'_{b,k} \nu_{b,k}, \quad (22d)$$

$$- \|\{\boldsymbol{\delta}_{b,k}^i \mathbf{M}_b\}^H\|_2 + [\boldsymbol{\mu}_{b,k}]_i \geq 0, i = 1 \dots l_{b,k}, \forall b, k, \quad \|\boldsymbol{\mu}_{b,k}\| \leq \nu_{b,k}, \forall b, k \quad (22e)$$

$$\|\text{vec}(\mathbf{M}_b)\|_2 \leq \sqrt{P_b}, \quad \forall b \quad (22f)$$

where $\mathbf{m}_k \in \mathbb{C}^{T \times 1}$, $\mathbf{M}_b = [\mathbf{m}_{\mathcal{U}_b(1)}, \dots, \mathbf{m}_{\mathcal{U}_b(|\mathcal{U}_b|)}]$, $z_{b,k} \in \mathbb{R}$, $L_{b_k,k} \in \mathbb{R}$, $\nu_{b,k} \in \mathbb{R}$, $\mathbf{q}_{b_k,k} \in \mathbb{C}^{l_{b_k,k}}$, $\boldsymbol{\mu}_{b,k} \in \mathbb{C}^{l_{b,k}}$ are optimization variables. The above optimization problem represents a tractable approximation, in the form of SOCP in conjunction with bisection search, of the robust counterpart of the problem under consideration. In the following, we provide some remarks regarding the tractability and reduced complexity of the proposed SOCP-based robust design.

Tractability: We emphasize that while the SDP-based solution is only applicable to ellipsoidal uncertainty models, the SOCP-based approach is flexible enough to deal with other types of uncertainty sets. For example, in certain situations, the errors in each of the individual terms of the channel vector are bounded i.e., $|\mathbf{v}_{b,k}|_i \leq \xi_{b,k}$ for all b, k, i . This amounts to saying that $\|\mathbf{v}_{b,k}\|_\infty \leq \xi_{b,k}$. In fact, in practical systems where each entry of $\mathbf{h}_{b,k}$ is quantized independently at the receiver and fed back to the corresponding transmitters, the interval uncertainty model is more appropriate [22]. Clearly, this uncertainty model can be easily handled with the above approach since the dual of the l_∞ norm is well known [8]. In other situations, it may happen that the entries of the uncertainty vector are symmetrically random and bounded. In such scenarios it is well known that the perturbation set can be represented as the intersection of the l_2 and l_∞ norms of $\mathbf{v}_{b,k}$ [23]. For this uncertainty model, it may be difficult, if not impossible, to straightforwardly use worst case design philosophy. Hence, the SDP-based method is not applicable and problem (7) appears to be intractable. However, the SOCP-based approach admits tractability in the approximate solution of the robust counterpart using the dual of the $l_2 \cap l_\infty$ norm [23].

Complexity Reduction: The SOCP-based robust design also offers a great reduction in compu-

tational complexity compared to the SDP-based method. In what follows, we give a complexity comparison of the SDP- and SOCP-based solutions for the special case where $\mathbf{A}_{b,k} = \mathbf{I}_T$ for all b, k , which is commonly considered in the related works.² First, let us focus on the equivalent representation obtained using Theorem 1 and explore it by considering any robust equivalent constraint (without loss of generality) from (22e). We note that under this setting each entry of a channel can be written as $[\mathbf{h}_{b,k}]_m = [\hat{\mathbf{h}}_{b,k}]_m + [\boldsymbol{\delta}_{b,k}]_m [\mathbf{v}_{b,k}]_m$, $1 \leq m \leq T$, where $\mathbf{v}_{b,k}$ belongs to the uncertainty set defined in (8). The vector $\boldsymbol{\gamma}_{b,k}$ corresponding to the equivalent formulation of Theorem 1 becomes

$$\boldsymbol{\gamma}_{b,k}^T = [|[\mathbf{m}_{\mathcal{U}_b(1)}]_m [\boldsymbol{\delta}_{b,k}]_m|, \dots, |[\mathbf{m}_{\mathcal{U}_b(|\mathcal{U}_b|)}]_m [\boldsymbol{\delta}_{b,k}]_m|], \forall b, k. \quad (23)$$

With this type of $\boldsymbol{\gamma}_{b,k}$ it has been shown in [15] that for ellipsoidal uncertainty set, instead of having multiple additional constraints of the type mentioned above, we can stack all corresponding variables into one SOC constraint, $\|\boldsymbol{\mu}_{b,k}\|_2 \leq \nu_{b,k}$, and one variable $\nu_{b,k}$ for all b, k . Similarly, the constraints involving user (b_k, k) , shown in (22b)-(22c), can be greatly simplified.

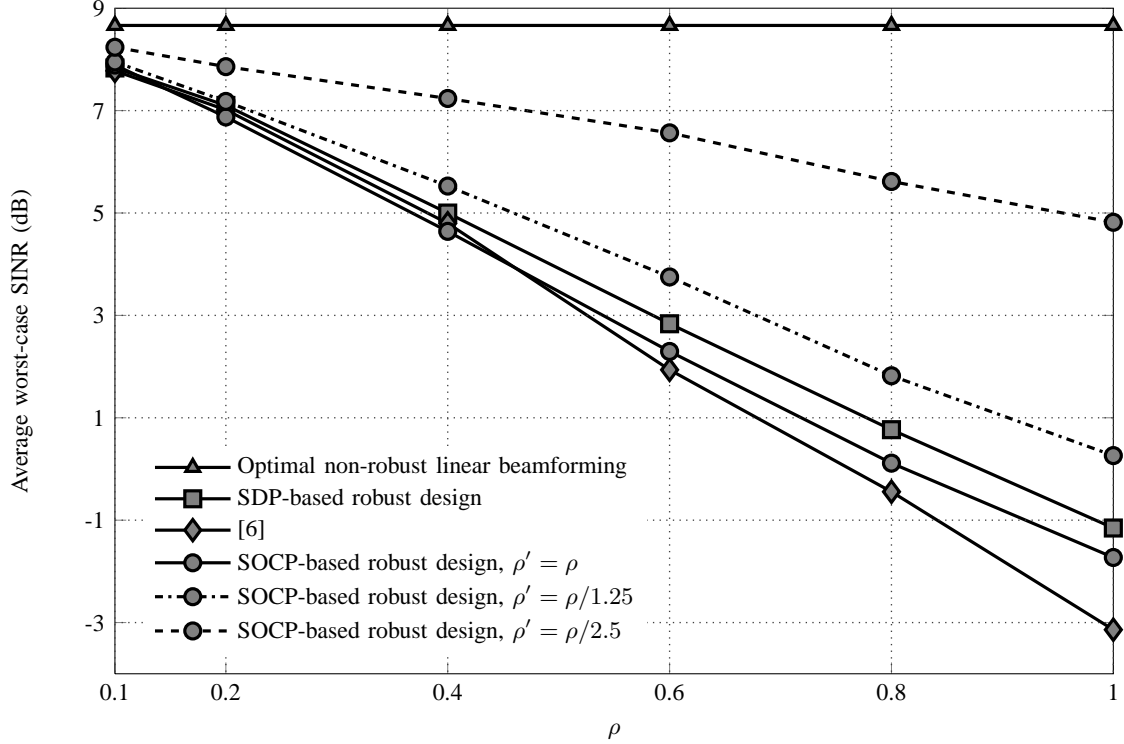
To provide a complexity comparison, we base our discussion on the simplification noted above and focus on an arbitrary bisection step. According to (22a)-(22f), the number of real optimization variables per bisection iteration of the SOCP-based robust design is $4TBK + 2BK + 2KT + K$. More specifically, there are BK constraints of real dimension $(2TK_b + 1)$ that occur thrice including the power constraint. Again using the above mentioned simplification, we obtain two constraints of real dimensions $B + 2$ and $T + 1$ that are K in number. Combining all these the worst case per iteration complexity of the SOCP approach approximates as $\mathcal{O}(K_b(TBK)^3)$ [24], [25]. The per iteration complexity of the SDP-based method is found to be $\mathcal{O}((KBT)^6)$ [24], [26], which is clearly higher than the SOCP counterpart. Further to this, based on [24], [25], the worst case estimate of the number of iterations needed to arrive at a numerically acceptable value of the SOCP-based design is $\mathcal{O}(\sqrt{KB})$. As similar calculation reveals that such an estimate for the SDP-based method results in a higher value of $\mathcal{O}(\sqrt{KTB})$ on account of its dependence on the size of the matrix inequalities. A more detailed exploration that compares run times of the proposed approaches with different solvers is given in Sec. IV.

²The same arguments in this part also apply to case where the entries of channel vectors undergo independent perturbations.

IV. NUMERICAL RESULTS

In order to compare the performance of the proposed approaches we report results of numerical simulations in this section. For all simulation setups, we consider a system of two cells ($B = 2$), while the number of users per cell is mentioned for individual numerical experiments. The channel vector from the BS b to user k is given by $\mathbf{h}_{b,k} = \sqrt{\kappa_{b,k}} \tilde{\mathbf{h}}_{b,k}$ where $\kappa_{b,k}$ represents both the path loss and the shadow fading and $\tilde{\mathbf{h}}_{b,k}$ follows $\mathcal{CN}(0, \mathbf{I})$. In Figs. 2-4 to follow, we only consider the small-scale fading (i.e., $\kappa_{b,k} = 1$ for all b and k). These setups can be considered to correspond to the worst-case scenario where all users are at the cell edge. A more realistic channel model where large-scale fading is taken into account is investigated in Fig. 5 for a massive MISO system. All noise variances are taken as unity and the transmit power is normalized with respect to the noise variance. For the sake of simplicity, but without compromising generality, we take $\alpha_k = 1$ for all k , $\mathbf{A}_{b,k} = \mathbf{I}_T$, and $\rho_{b,k} = \rho$ for all b, k . Unless otherwise mentioned, the error vectors are assumed to lie in a hypersphere of radius ρ . We evaluate the performance of the three approaches in terms of the worst-case SINR (i.e., the objective obtained at the end of the bisection procedure when solving (9) and (22)) and the probability of exceeding the worst-case SINR which is referred to as PE from now on. For the simulation setup considered in this paper, the SDP-based approach is numerically found to produce precoding matrices close to rank-1 matrices.

Fig. 2 plots the average worst-case SINRs (over 200 realizations of the nominal channels $\hat{\mathbf{h}}_{b,k}$) versus the radius of the uncertainty sets, ρ , for all approaches. In this simulation setup, we only consider the small-scale fading (i.e., $\kappa_{b,k} = 1$ for all b and k). The number of users in each BS is 2, i.e., there are $K = 4$ users in total. It is seen in Fig. 2(a) that the SOCP-based solution gives the worst-case SINR close to that of the SDP-based approach and slightly higher than that of [6] when $\rho' = \rho$. As mentioned earlier, by taking ρ' as a design parameter, we can achieve a trade-off between the worst-case SINR and the resulting PE. It can be seen from Fig. 2 that the worst-case SINR of the SOCP-based solution is improved when we take $\rho' = \rho/2.5$, but this implies reduced PE as indicated in table 2(b). The values of PE given in table 2(b) are obtained with 10^6 sets of channel errors that are uniformly distributed in the ball of ρ using the toolbox of [27]. As expected, the non-robust approach delivers the maximum SINR and virtually zero PE in all cases.



(a) Average worst-case SINR versus ρ .

ρ	0.1	0.2	0.4	0.6	0.8	1
PE non-robust	0	0	0	0	0	0
PE SDP	1	1	1	1	1	1
PE [6]	1	1	1	1	1	1
PE ($\rho' = \rho$)	1	1	1	1	1	1
PE ($\rho' = \rho/1.25$)	0.99	1	0.99	0.99	0.98	0.99
PE ($\rho' = \rho/2.5$)	0.81	0.87	0.82	0.75	0.80	0.73

(b) Variation of PE with ρ for the proposed SOCP-based robust design.

Fig. 2. Average worst-case SINR versus ρ for different approaches where channel uncertainties are bounded by l_2 -norm. The value of power for both BSs is taken as 5 dB. The number of transmit antennas at each BS is $T = 8$. The total number of users is $K = 4$ (2 users per base station).

Although the SDP formulations can offer better worst-case SINR, they are not practically useful for large-scale antenna systems especially from the complexity perspective. Another disadvantage of the SDP approach is its inability to handle various uncertainty sets and limited choice of solvers compared to those for SOCP based solutions. The flexibility in choosing a solver is important because a general purpose convex programming solver may not be efficient for all problems. We compare the simulation time of the SDP and SOCP-based robust designs

TABLE I

THE AVERAGE RUN TIME (IN SECONDS) VERSUS THE NUMBER OF TRANSMIT ANTENNAS, T , AT EACH BS FOR THE ROBUST DESIGNS. THE NUMBER OF BSs IS $B = 2$, EACH SERVING 10 USERS. THE BISECTION PROCEDURE TERMINATES WHEN THE DIFFERENCE BETWEEN THE OBJECTIVE VALUES OF TWO BISECTION STEPS, $\epsilon \leq 10^{-2}$.

Antennas	8	12	16	50	100	200	300	400	500
SDP-based design (SDPT3) (sec)	96.48	477.55	5620.3397	×	×	×	×	×	×
SDP-based design (SeDuMi) (sec)	31.44	162.68	684.57	×	×	×	×	×	×
[6] (SDPT3) (sec)	88.34	130.83	240.33	×	×	×	×	×	×
[6] (SeDuMi) (sec)	48.01	61.09	156.78	×	×	×	×	×	×
SOCP-based design (SDPT3) (sec)	1.63	4.04	4.07	28.09	99.23	285.74	—	—	—
SOCP-based design (SeDuMi) (sec)	0.66	1.09	1.23	21.92	51.31	149.68	—	—	—
SOCP-based design (GUROBI) (sec)	1.08	1.95	2.14	12.02	23.66	44.91	47.37	67.46	90.72

using YALMIP [28] with two widely used conic programming solvers (SeDuMi [29] and SDPT3 [30]). Note that the proposed SOCP-based method allows us to make use of GUROBI [31] as a solver as well which is claimed to be very efficient for detecting feasibility of large-scale SOCPs. For the robust SOCP-based design, we use the simplified representation in (23). In Table I, we show the average run time (in seconds) of all robust approaches as a function of the number of transmit antennas, T , for solving the corresponding optimization problem. The bisection procedure terminates if feasibility is detected and the relative difference ϵ of the objectives between two bisection steps is less than or equal to 10^{-2} . The lower threshold of the bisection algorithm is set to 0, while the upper one is equal to the balanced SINR obtained from the non-robust design. The codes are executed on a 64-bit desktop that supports 8 Gbyte RAM and Intel CORE i7. For both solvers, it can be clearly seen that the SOCP-based design requires a lower run time and the difference is considerable as the number of transmit antennas T increases. This observation matches with the theory presented in the subsection on reduced complexity in Sec. III-B. Moreover, we notice that the SDP-based methods are not capable of producing a solution when $T \geq 50$ due to lack of memory (denoted by a cross mark “×” in Table I). When $T \geq 300$, SeDuMi and SDPT3 are not suitable solvers for the SOCP-based method since they are not able to produce a solution even after several hours (denoted by “—” in Table I). We have observed that GUROBI is the most efficient solver for the SOCP-based method in particular for large-scale antenna array systems.

In Fig. 3, the average worst-case balanced SINR (again over 200 realizations of the nominal channels $\hat{\mathbf{h}}_{b,k}$) is plotted with the transmit power per BS, P , for different approaches. We note that the SOCP-based approach performs nearly as good as the SDP one. The reduced minimum SINR

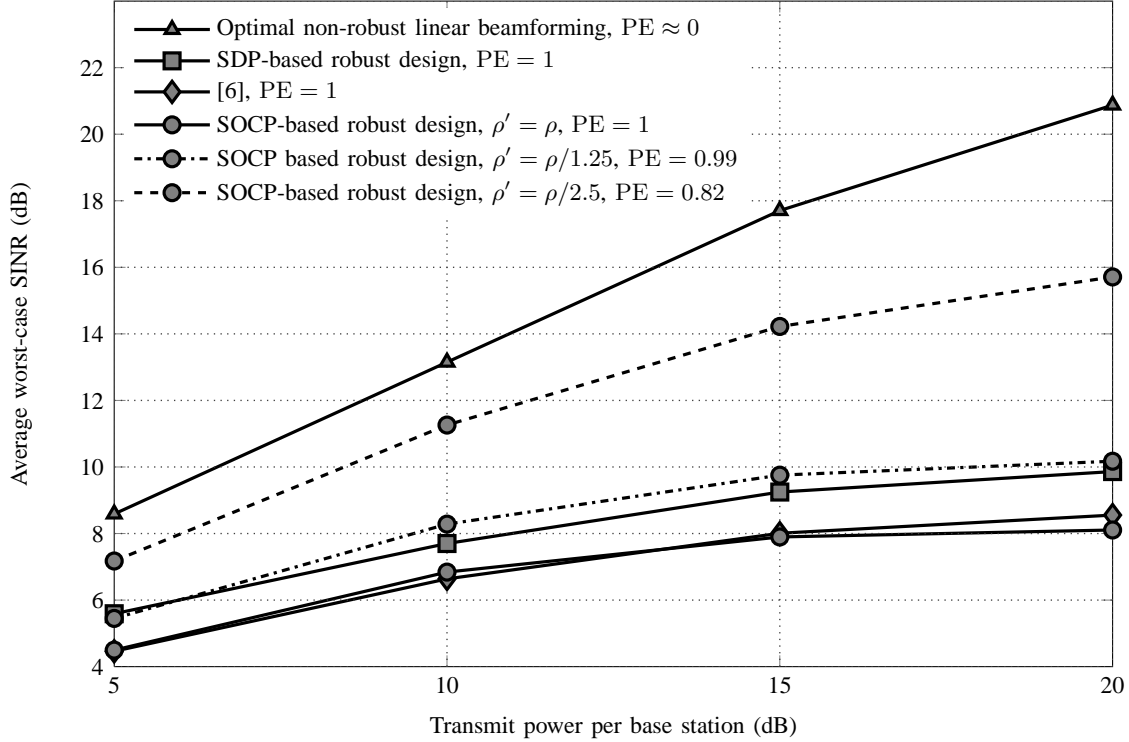
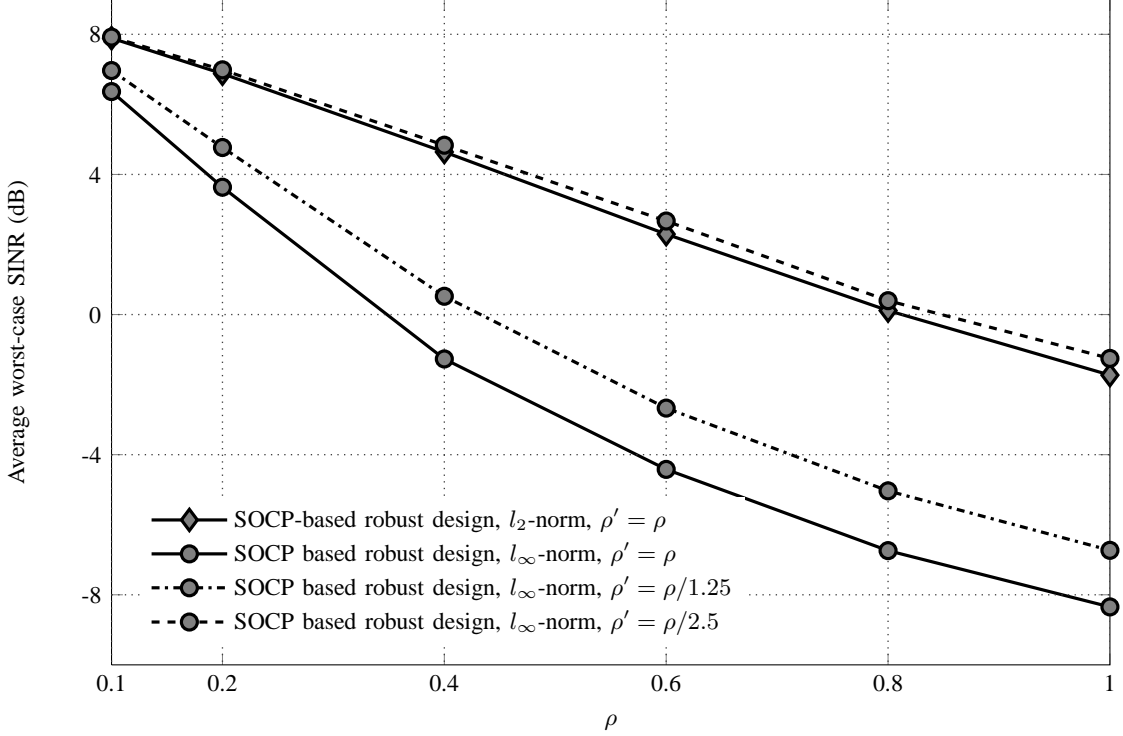


Fig. 3. Comparison of the worst-case SINR of non-robust, SOCP-, SDP-based design, and the approach of [6] as a function of the transmit power of the BSs for $\rho = 0.4$. The performances of the SOCP-based method are shown for three cases where $\rho' = \rho$, $\rho' = \rho/1.25$ and $\rho' = \rho/2.5$.

of [6] can be probably attributed to the fact that it is completely a conservative approximation of the robust counterpart. Recall that, in our proposed SOCP-based design, we can control the degree of conservatism of the design by finding proper value of ρ' . The values of PE for three approaches are also provided in Fig. 3. Further, being oblivious to channel error vectors, the non robust design delivers the best worst-case SINR. Nonetheless, as expected and seen previously, this comes at the cost of unacceptably low PE, i.e., $PE \approx 0$. It is found that the SOCP-based method gives $PE = 0.99$ for $\rho' = \rho/1.25$, while the approach of [6] and the SDP-based solution both produce $PE = 1.0$. The value of PE for the SOCP-based design is reduced to 0.82 as we set $\rho' = \rho/2.5$. Interestingly, this decrease in PE is accompanied by a corresponding increase in the worst-case SINR, thereby providing a tradeoff between the two parameters. We note that the trend of values of PE is observed to be typical for the range of transmit power considered in Fig. 3.

In Fig. 4 we evaluate performance of robust beamforming for SINR balancing where the



(a) Variation of average worst-case SINR versus ρ for l_∞ -norm.

ρ	0.1	0.2	0.4	0.6	0.8	1
PE ($\rho' = \rho$)	1	1	1	1	0.96	0.98
PE ($\rho' = \rho/1.25$)	1	1	0.99	0.99	0.95	0.97
PE ($\rho' = \rho/2$)	1	0.97	0.96	0.95	0.95	0.91
PE ($\rho' = \rho/2.5$)	0.8	0.88	0.81	0.81	0.81	0.80

(b) Variation of PE with ρ for l_∞ -norm for the proposed SOCP-based robust approach.

Fig. 4. Variation of average worst-case SINR versus ρ for l_∞ -norm (i.e., “box” uncertainty). The value of power for both BSs has been taken as 5 dB. The number of transmit antennas at each BS is $T = 8$. The total number of users is $K = 4$.

errors in elements of channel vectors are bounded within a (multi-dimensional) box of size ρ , i.e., $|\mathbf{v}_{b,k}|_i \leq \rho$ for all i . This is equivalent to saying that $\|\mathbf{v}_{b,k}\|_\infty \leq \rho$. For this case, we note that the SDP formulations and the approximations used in [6] are not applicable. The curves in Fig. 4 have been obtained by noting the fact that the dual of l_∞ -norm is l_1 -norm. It is seen that, with box uncertainty (Fig. 4), the worst-case SINR is lower than that in the case of ellipsoidal uncertainty for the same ρ . This can be explained as follows. We note that for a vector \mathbf{v} , $\|\mathbf{v}\|_1 \geq \|\mathbf{v}\|_2 \geq \|\mathbf{v}\|_\infty$, which means that for the same ρ , the l_∞ -norm defines a smaller feasible set in (22) compared to the l_2 -norm. Thus the worst-case SINR for the l_∞ -norm uncertainty is

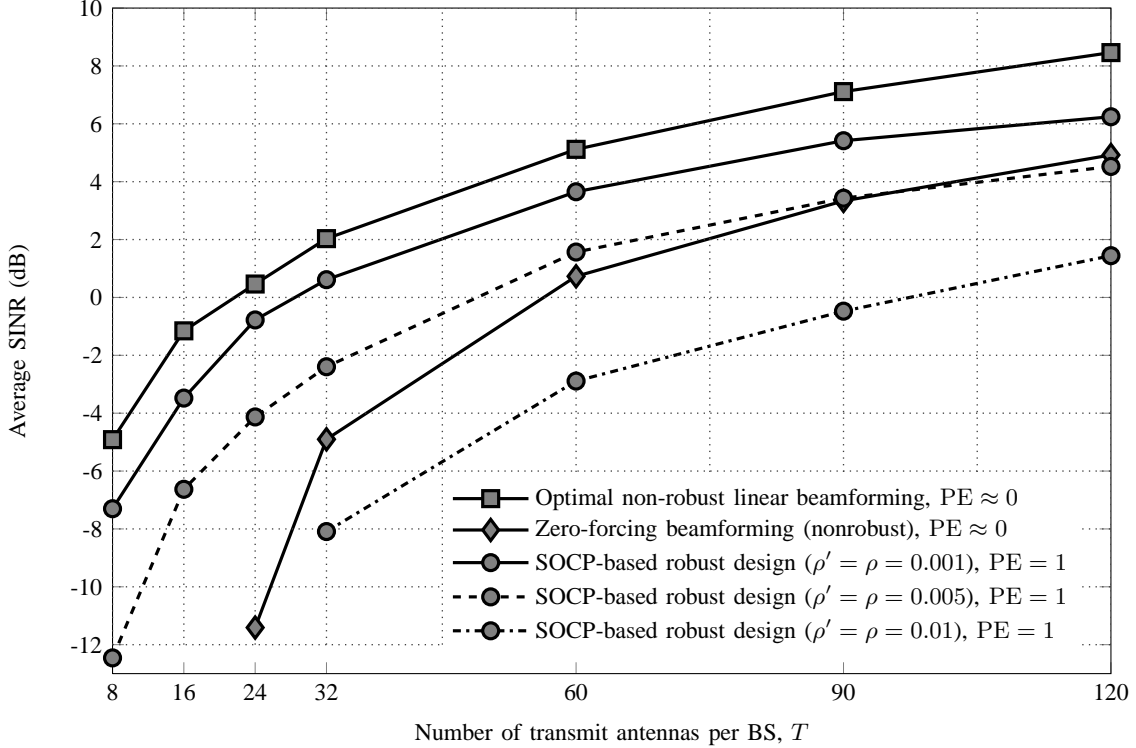


Fig. 5. Variation of average balanced SINR versus the number of transmit antennas per BS, T . For robust designs, channel uncertainties are bounded in a ball of radius ρ . The value of the normalized power for both BSs is taken as 20 dB. The total number of users is $K = 20$ (10 users per cell).

lower than that of the l_2 -norm. However, when errors are uniformly distributed in a box, we note in the table given in Fig. 4(b) a slight degradation in PE when $\rho' = \rho$. This stems from the fact that the proposed approach is not guaranteed to be safe as discussed earlier in the paper.

Finally, in Fig. 5 we investigate how the balanced SINR of all users scales with the number of transmit antennas. In particular, we consider a system of two cells, each serving 10 users. The users are uniformly distributed in the cell and are not allowed to be closer to the BS by more than $d_0 = 100$ meters [32]. We also assume that the cell diameter (to a vertex) is 1000 meters. The large-scale fading coefficient is modeled as $\kappa_{b,k} = \beta_{b,k}(d_{b,k}/d_0)^{-\nu}$ where $\beta_{b,k}$ accounts for shadow fading assumed to follow a log-normal distribution with standard deviation σ_{shadow} , ν is the path loss exponent, and $d_{b,k}$ is the distance between BS b and user k . In Fig. 5, we choose $\sigma_{\text{shadow}} = 8$ dB and $\nu = 3.8$ as in [32]. In Fig. 5, the performance of zero-forcing beamforming (ZF-BF) scheme is also included for comparison. In ZF-BF, multiuser interference for each user is forced to zero, i.e., $\mathbf{h}_{b_i,j}\mathbf{m}_i = 0$ for all $j \neq i$ [33], [34]. In this way, problem (4) is simplified

as

$$\underset{(t, \mathbf{m}_k) \in \mathcal{F}}{\text{maximize}} \quad t \quad (24)$$

where $\mathcal{F} \triangleq \{(t, \mathbf{m}_k) \mid \mathbf{h}_{b_i, j} \mathbf{m}_i = 0, \forall i \neq j, \|\mathbf{M}_b\|_2 \leq \sqrt{P_b}, \forall b, \sigma_{\alpha_k} \leq \Re(\mathbf{h}_{b_k, k} \mathbf{m}_k), \forall k\}$ which is convex. Consequently, problem (24) is jointly convex in t and \mathbf{m}_k . Using the null-space technique as devised in [33], [34], we can further remove the ZF constraints $\mathbf{h}_{b_i, j} \mathbf{m}_i = 0, \forall i \neq j$ in \mathcal{F} without loss of optimality as follows. Let $\bar{\mathbf{M}}_k = [\mathbf{h}_{b_1, k}^T \quad \mathbf{h}_{b_2, k}^T \quad \cdots \quad \mathbf{h}_{b_{k-1}, k}^T \quad \mathbf{h}_{b_{k+1}, k}^T \quad \cdots \quad \mathbf{h}_{b_K, k}^T]^T \in \mathbb{C}^{(K-1) \times T}$ and $\mathbf{G}_k \in \mathbb{C}^{T \times (T-K+1)}$ be a matrix of orthogonal columns that span the null space of $\bar{\mathbf{M}}_k$.³ Then, to satisfy the ZF constraints, we can write $\mathbf{m}_k = \mathbf{G}_k \tilde{\mathbf{m}}_k$. The problem (24) is thus further equivalent to

$$\underset{(t, \tilde{\mathbf{m}}_k) \in \tilde{\mathcal{F}}}{\text{maximize}} \quad t \quad (25)$$

where $\tilde{\mathbf{h}}_{b_k, k} \triangleq \mathbf{h}_{b_k, k} \mathbf{G}_k$ and $\tilde{\mathbf{M}}_b \triangleq [\tilde{\mathbf{m}}_{U_b(1)}, \dots, \tilde{\mathbf{m}}_{U_b(|U_b|)}]$ and $\tilde{\mathcal{F}} \triangleq \{\tilde{\mathbf{m}}_k \mid \|\tilde{\mathbf{M}}_b\|_2 \leq \sqrt{P_b} \forall b, \sigma_{\alpha_k} \leq \Re(\tilde{\mathbf{h}}_{b_k, k} \tilde{\mathbf{m}}_k), \forall k\}$. The advantage of the ZF-BF scheme is that we can avoid the bisection procedure that must be carried out to solve (4) for optimal linear beamforming. However, even for perfect CSI, the performance of ZF-BF is still far away from that of optimal linear beamforming as shown in Fig. 5. For example, when $T = 120$, a gap of about 4 dB is observed between ZF-BF and general linear beamforming. These non-robust designs are sensitive to channel errors as shown by the fact that PE ≈ 0 for both these cases. The benefit of using large-scale antenna systems is seen in Fig. 5, when a gain of 13 dB is observed as the number of transmit antennas is increased from $T = 8$ to $T = 120$ for optimal linear beamforming with perfect CSI. A similar conclusion also applies to the robust designs when ρ is taken as 0.001, 0.005 and 0.01. We note that these values of ρ are comparable to the average channel gains of $\mathbf{h}_{b, k}$ taking into account the effect of shadowing and path loss. Therefore, owing to the conservative nature of robust designs it is not possible to achieve nontrivial SINRs for higher values of ρ .

V. CONCLUSION

We have studied the design of beamformers that balance the SINR of users in a multicell downlink system in the presence of channel uncertainties. Norm bounded channel uncertainty model is used. As a first approach to solving the problem in this scenario, we present an S-

³For the ZF-BF scheme to be feasible, i.e., $\dim(\mathbf{G}_k) > 0$, we must have $T \geq K$.

lemma based approximate solution in which the beamformers are obtained by solving an SDP in conjunction with bisection search. Later, by exploiting various properties of the functions involved in the problem, we present a solution in which robust beamformers are solutions to an SOCP-based formulation. We show that in addition to being capable of handling different uncertainty sets, the SOCP-based approximation exhibits a much reduced complexity solution. We have tested the performance of proposed approaches for the recently conceived massive antenna systems, and have determined that the SOCP approach outperforms the SDP-based solution from computational cost perspective. Finally, we have also shown that the reduced complexity SOCP-based approach yields a balanced SINR and the probability of achieving it which is comparable with the SDP approach.

ACKNOWLEDGMENT

The authors would like to thank Prof. Johan Löfberg of the Linköping University, Sweden for his helpful advice regarding the numerical results presented in the paper.

APPENDIX

PROOF OF THEOREM 1

We will follow the notation in (19) and obtain a tractable version of this constraint by adapting the arguments developed in [15]. Let O_1 and O_2 be the optimal solutions of

$$\max \quad \mathbf{a}_1^T \mathbf{v}_1 + \mathbf{a}_2^T \mathbf{v}_2 \quad (26a)$$

$$\text{subject to} \quad \|\mathbf{v}_1 + \mathbf{v}_2\| \leq \vartheta \quad (26b)$$

$$\mathbf{v}_1 \geq 0, \mathbf{v}_2 \geq 0. \quad (26c)$$

and

$$\max \quad \sum_{i \in \mathcal{I}} \max\{[\mathbf{a}_1]_i, [\mathbf{a}_2]_i, 0\} [\mathbf{v}_3]_i \quad (27a)$$

$$\text{subject to} \quad \|\mathbf{v}_3\| \leq \vartheta. \quad (27b)$$

respectively. It is shown in [15] that $O_1 = O_2$. Now consider the following set of relations that can be obtained from (19), i.e.,

$$f_1(\mathbf{M}_b, z_{b,k}, \hat{\mathbf{h}}_{b,k}) \geq - \min_{\|\boldsymbol{\theta}_{b,k}\| + \|\boldsymbol{\Phi}_{b,k}\| \leq \rho'_{b,k}} \sum_{i=1}^{l_{b,k}} \left\{ f_2(\mathbf{M}_b, \boldsymbol{\delta}_{b,k}^i) |[\boldsymbol{\theta}_{b,k}]_i| + f_2(\mathbf{M}_b, -\boldsymbol{\delta}_{b,k}^i) |[\boldsymbol{\Phi}_{b,k}]_i| \right\} \quad (28a)$$

$$= \max_{\|\boldsymbol{\theta}_{b,k}\| + \|\boldsymbol{\Phi}_{b,k}\| \leq \rho'_{b,k}} \sum_{i=1}^{l_{b,k}} \left\{ -f_2(\mathbf{M}_b, \boldsymbol{\delta}_{b,k}^i) |[\boldsymbol{\theta}_{b,k}]_i| - f_2(\mathbf{M}_b, -\boldsymbol{\delta}_{b,k}^i) |[\boldsymbol{\Phi}_{b,k}]_i| \right\} \quad (28b)$$

$$= \max_{\|\mathbf{v}_{3b,3k}\| \leq \rho'_{b,k}} \sum_{i=1}^{l_{b,k}} \left\{ \max \left(-f_2(\mathbf{M}_b, \boldsymbol{\delta}_{b,k}^i), -f_2(\mathbf{M}_b, -\boldsymbol{\delta}_{b,k}^i), 0 \right) |[\mathbf{v}_{3b,3k}]_i| \right\} \quad (28c)$$

where in (28c) we have employed the result in optimization problem formulation (27), and have slightly changed the representation in (19) by not specifying any particular norm in the constraint set. Now recalling the definition of the dual norm $\vartheta \|\boldsymbol{\gamma}\|^* \triangleq \max_{\|\mathbf{s}\| \leq \vartheta} \mathbf{s}^T \boldsymbol{\gamma}$ of vector $\boldsymbol{\gamma}$, we obtain the result stated in Theorem 1 for the constraint set of interest.

REFERENCES

- [1] J. Jose, A. Ashikhmin, T. L. Marzetta, and S. Vishwanath, "Pilot contamination and precoding in multi-cell TDD systems," *IEEE Trans. Wireless Commun.*, vol. 10, no. 8, pp. 2640–2651, Aug. 2011.
- [2] H. A. Suraweera, P. J. Smith, and M. Shafi, "Capacity limits and performance analysis of cognitive radio with imperfect channel knowledge," *IEEE Trans. Veh. Technol.*, vol. 59, no. 4, pp. 1811–1822, May 2010.
- [3] S. A. Vorobyov, A. B. Gershman, and Z.-Q. Luo, "Robust adaptive beamforming using worst-case performance optimization: a solution to the signal mismatch problem," *IEEE Trans. Signal Process.*, vol. 51, no. 2, pp. 313–324, Feb. 2003.
- [4] N. Vucic and H. Boche, "Robust QoS-constrained optimization of downlink multiuser MISO systems," *IEEE Trans. Signal Process.*, vol. 57, no. 2, pp. 714–725, Feb. 2009.
- [5] G. Zheng, K. K. Wong, and B. Ottersten, "Robust cognitive beamforming with bounded channel uncertainties," *IEEE Trans. Signal Process.*, vol. 57, no. 12, pp. 4871–4881, Dec. 2009.
- [6] A. Tajer, N. Prasad, and X. Wang, "Robust linear precoder design for multi-cell downlink transmission," *IEEE Trans. Signal Process.*, vol. 59, no. 1, pp. 235–251, Jan. 2011.
- [7] D. Bertsimas, D. B. Brown, and C. Caramanis, "Theory and applications of robust optimization," *SIAM Rev.*, vol. 53, no. 3, pp. 464–501, 2011.
- [8] A. B. Tal, L. E. Ghaoui, and A. Nemirovski, *Robust Optimization*. Princeton, USA: Princeton University Press, Aug. 2009.
- [9] F. Rusek, D. Persson, B. K. Lau, E. Larsson, T. L. Marzetta, O. Edfors, and F. Tufvesson, "Scaling up MIMO: Opportunities and challenges with very large arrays," *IEEE Signal Process. Mag.*, vol. 30, no. 1, pp. 40–60, Jan. 2013.

- [10] L. Tran, M. F. Hanif, A. Tolli, and M. Juntti, "Fast converging algorithm for weighted sum rate maximization in multicell MISO downlink," *IEEE Signal Process. Lett.*, vol. 19, no. 12, pp. 872–875, Dec. 2012.
- [11] A. Tolli, M. Codreanu, and M. Juntti, "Linear multiuser MIMO transceiver design with quality of service and per-antenna power constraints," *IEEE Trans. Signal Process.*, vol. 56, no. 7, pp. 3049–3055, July 2008.
- [12] A. Wiesel, Y. C. Eldar, and S. Shamai, "Linear precoding via conic optimization for fixed MIMO receivers," *IEEE Trans. Signal Process.*, vol. 54, no. 1, pp. 161–176, Jan. 2006.
- [13] S. Boyd and L. Vandenberghe, *Convex Optimization*. Cambridge, U. K.: Cambridge University Press, 2004.
- [14] A. B. Tal and A. Nemirovski, "Robust convex optimization," *Mathematics of Operations Research*, vol. 23, no. 4, pp. 769–805, Nov. 1998.
- [15] D. Bertsimas and M. Sim, "Tractable approximations to robust conic optimization problems," *Mathematical Programming*, vol. 107, no. 1-2, pp. 5–36, 2006.
- [16] T. Yoo and A. Goldsmith, "Capacity and power allocation for fading MIMO channels with channel estimation error," *IEEE Trans. Inf. Theory*, vol. 52, no. 5, pp. 2203–2214, May 2006.
- [17] J. Zheng, E. Duni, and B. Rao, "Analysis of multiple-antenna systems with finite-rate feedback using high-resolution quantization theory," *IEEE Trans. Signal Process.*, vol. 55, no. 4, pp. 1461–1476, Apr. 2007.
- [18] S. Boyd, L. E. Ghaoui, E. Feron, and V. Balakrishnan, *Linear Matrix Inequalities in Systems and Control Theory*. Philadelphia, PA: SIAM, 1994.
- [19] E. Song, Q. Shi, M. Sanjabi, R. Sun, and Z.-Q. Luo, "Robust SINR-constrained MISO downlink beamforming: When is semidefinite programming relaxation tight?" in *Proc. IEEE International Conference on Acoustics, Speech and Signal Processing (ICASSP)*, May 2011, pp. 3096–3099.
- [20] Z.-Q. Luo, W. K. Ma, A. M.-Cho, Y. Ye, and S. Zhang, "Semidefinite relaxation of quadratic optimization problems," *IEEE Signal Process. Mag.*, vol. 27, no. 3, pp. 20–34, May 2010.
- [21] D. Bertsimas and D. B. Brown, "Constrained stochastic LQC: A tractable approach," *IEEE Trans. Autom. Control*, vol. 52, no. 10, pp. 1826–1841, Oct. 2007.
- [22] M. Shenouda and T. Davidson, "Nonlinear and linear broadcasting with QoS requirements: Tractable approaches for bounded channel uncertainties," *IEEE Trans. Signal Process.*, vol. 57, no. 5, pp. 1936–1947, May 2009.
- [23] A. B. Tal and A. Nemirovski, "Robust solutions of linear programming problems contaminated with uncertain data," *Math. Progr.*, vol. 88, no. 3, pp. 411–424, July 2000.
- [24] L. Vandenberghe and S. Boyd, "Semidefinite programming," *SIAM Rev.*, vol. 38, no. 1, pp. 49–95, Mar. 1996.
- [25] M. S. Lobo, L. Vandenberghe, S. Boyd, and H. Lebret, "Applications of second-order cone programming," *Linear Algebra Applications, Special Issue on Linear Algebra in Control, Signals and Image Processing*, pp. 193–228, Nov. 1998.
- [26] Z.-Q. Luo, T. N. Davidson, G. B. Giannakis, and K. M. Wong, "Transceiver optimization for block-based multiple access through ISI channels," *IEEE Trans. Signal Process.*, vol. 52, no. 4, pp. 1037–1052, April 2004.
- [27] A. Tremba, G. Calafiore, F. Dabbene, E. Gryazina, B. Polyak, P. Shcherbakov, and R. Tempo, "RACT: Randomized algorithms control toolbox for MATLAB," in *Proc. the 17th World Congress The International Federation of Automatic Control (IFAC)*, Seoul, Korea, 2008. [Online]. Available: <http://ract.sourceforge.net>
- [28] J. Löfberg, "YALMIP : A toolbox for modeling and optimization in MATLAB," in *Proc. the CACSD Conference*, Taipei, Taiwan., 2004. [Online]. Available: <http://users.isy.liu.se/johanl/yalmip>
- [29] J. F. Sturm, "Using SeDuMi 1.02, a MATLAB toolbox for optimization over symmetric cones," *Optimization Methods and Software*, vol. 11–12, pp. 625–653, 1999.

- [30] K. C. Toha, M. J. Todd, and R. H. Tutuncuc, "SDPT3-a Matlab software package for semidefinite programming, version 1.3," *Optimization Methods and Software*, vol. 11, no. 1-4, pp. 545–581, 1999.
- [31] Gurobi Optimizer Version 5.1. Houston, Texas: Gurobi Optimization, Mar., April 2013. [Online]. Available: <http://www.gurobi.com/>
- [32] H. Q. Ngo, E. G. Larsson, and T. L. Marzetta, "Energy and spectral efficiency of very large multiuser MIMO systems," *IEEE Trans. Commun.*, to appear. [Online]. Available: <http://arxiv.org/abs/1112.3810>
- [33] L.-N. Tran, M. Bengtsson, and B. Ottersten, "Iterative precoder design and user scheduling for block-diagonalized systems," *IEEE Trans. Signal Process.*, vol. 60, no. 7, pp. 3726–3739, Jul. 2012.
- [34] L.-N. Tran, M. Juntti, M. Bengtsson, and B. Ottersten, "Beamformer designs for MISO broadcast channels with zero-forcing dirty paper coding," *IEEE Trans. Wireless Commun.*, vol. 12, no. 3, pp. 1173–1185, Mar. 2013.